Helical axis stellarator equilibrium and resistive ballooning

M. C. Depassier
Facultad de Física, Universidad Católica de Chile, Casilla 114-D, Santiago, Chile

W. A. Cooper
Fusion Energy Division, Oak Ridge National Laboratory, P. O. Box Y, Oak Ridge, Tennessee 37831

(Received 15 October 1985; accepted 12 March 1986)

An approximate analytic solution of the magnetohydrodynamic (MHD) equilibrium equation for large-aspect-ratio, helically symmetric systems is obtained. The resistive ballooning stability of these equilibria is studied numerically and analytically. We find that the ballooning modes scale as the resistivity to the third power. They are driven by the helical nature of the magnetic axis and by the elliptic distortion of the flux surfaces away from a circle.

I. INTRODUCTION

A variety of plasma confinement configurations can be very adequately modeled by assuming that the magnetohydrodynamic (MHD) equilibrium properties satisfy helical symmetry.[1] This is the most general three-dimensional configuration that can be treated as two-dimensional because of its symmetry. For such systems we develop an approximate analytic solution to the MHD equilibrium equation. It has been shown that stellarator configurations that satisfy helical symmetry possess favorable ideal MHD stability properties.[2–6] Then stability, a three-dimensional problem, is simplified if we restrict ourselves to ballooning-mode stability, which, in an appropriate coordinate system, is reduced to the solution of an eigenvalue problem of an ordinary differential equation.[7,8] In this article we study the resistive ballooning stability of helically symmetric equilibria by numerical and analytical methods. We find that the growth rate of instability is given by Eq. (59), which compares well with the numerical results in the regime where such an expression is valid. In Sec. II we describe the geometry of systems with helical symmetry. In Sec. III we briefly rederive the MHD equilibrium for helically symmetric systems.[9] In Sec. IV an approximate analytic solution to this equation is obtained for large-aspect-ratio systems in a way analogous to that developed for toroidal systems.[10] In Sec. V we rederive the ballooning-mode equation[11] for helically symmetric systems, and in Sec. VI we obtain a reduced ballooning-mode equation valid for large-aspect-ratio equilibria. Finally, in Sec. VII an analytic formula for the growth rate of the instability is found by means of an asymptotic expansion. In Sec. VIII the numerical results are discussed. Brief concluding remarks are made in Sec. IX.

II. GEOMETRY

We consider plasma equilibrium configurations that have helical symmetry. Calling L the field period length, we choose the angular variable $u_3 = \phi = 2\pi Z/L$ as the coordinate of helical symmetry. Then, the divergence-free equilibrium magnetic field in contravariant representation may be written as

$$\mathbf{B} = \nabla\phi \times \nabla\psi + \sqrt{g} B^3 \nabla u_1 \times \nabla u_2 , \tag{1}$$

where $\psi = \psi(u_1, u_2)$ is the helical flux function, the Jacobian $\sqrt{g} = (\nabla u_1 \times \nabla u_2 \cdot \nabla u_3)^{-1}$, $B^3 = \mathbf{B} \cdot \nabla u_3$ is the longitudinal magnetic field, and u_1 and u_2 are arbitrary coordinates. A rotating Cartesian coordinate system, which we shall use to obtain an analytic solution of the MHD equilibrium equation, is defined through

$$u_1 = X = X_0 \cos\phi + Y_0 \sin\phi , \tag{2a}$$

$$u_2 = Y = -X_0 \sin\phi + Y_0 \cos\phi . \tag{2b}$$

The vector position in this coordinate system is $\mathbf{R} = X\nabla X + Y\nabla Y + Z\nabla Z$. Alternatively, we can also use a magnetic flux coordinate system, in which case we have $u_1 = \rho$, a radial variable that labels flux surfaces, and $u_2 = \theta$, the poloidal angle that sweeps along the flux surface. The Jacobian of the transformation from a fixed Cartesian coordinate system (X_0, Y_0, Z_0) to the rotating Cartesian coordinates (X, Y, ϕ) is $\sqrt{g} = 1/h$, and the Jacobian of the transformation from the rotating Cartesian coordinate system to the magnetic flux coordinate system (ρ, θ, ϕ) is given by $\sqrt{g} = (X_\rho Y_\theta - Y_\rho X_\theta)/h$. The covariant basis vectors are given by

$$\begin{aligned}\mathbf{e}_i &= \frac{\partial \mathbf{R}}{\partial u_i} \\ &= \left(\frac{\partial X}{\partial u_i} - Y\frac{\partial \phi}{\partial u_i}\right)\nabla X + \left(\frac{\partial Y}{\partial u_i} + X\frac{\partial \phi}{\partial u_i}\right)\nabla Y \\ &\quad + h^{-2}\left[\left[1 + h^2(X^2 + Y^2)\right]\frac{\partial \phi}{\partial u_i}\right. \\ &\quad \left. + h^2\left(X\frac{\partial Y}{\partial u_i} - Y\frac{\partial X}{\partial u_i}\right)\right]\nabla\phi ,\end{aligned} \tag{3}$$

and the contravariant basis vectors by

$$\mathbf{e}^i = \nabla u_i = \frac{\partial u_i}{\partial X}\nabla X + \frac{\partial u_i}{\partial Y}\nabla Y + \frac{\partial u_i}{\partial \phi}\nabla\phi . \tag{4}$$

The upper and lower metric elements are given by $g^{ij} = \mathbf{e}^i \cdot \mathbf{e}^j$ and $g_{ij} = \mathbf{e}_i \cdot \mathbf{e}_j$, respectively. Detailed expressions for them are given in Appendix A.

For stability studies, however, the most appropriate coordinate system is a straight magnetic flux coordinate system (ρ, θ_*, ϕ), where θ_* is that particular poloidal angle that makes the magnetic field lines straight. This coordinate system can be constructed from the knowledge of the equi-

 0031-9171/86/061948-11$01.90

librium magnetic field in arbitrary magnetic flux coordinates. In a magnetic flux coordinate system the flux function ψ depends only on ρ, so the equilibrium magnetic field is given by

$$\mathbf{B} = \nabla\phi \times \nabla\psi + \sqrt{g} B^3 \nabla\rho \times \nabla\theta . \tag{5}$$

In a straight magnetic field line coordinate system, $(\sqrt{g}B^3)$ does not depend on θ. Therefore, the longitudinal flux $\Phi = \int\int d\rho\, d\theta\, \sqrt{g}(\mathbf{B}\cdot\nabla\phi)$ is given by $\Phi = 2\pi \int d\rho\, \sqrt{g}(\mathbf{B}\cdot\nabla\phi)$, and the q factor is given by $q(\rho) = \sqrt{g}(\mathbf{B}\cdot\nabla\phi)/\psi'$, so that the magnetic field in the straight magnetic flux system is

$$\mathbf{B} = \nabla\phi \times \nabla\psi + q(\rho)\nabla\psi \times \nabla\theta_* . \tag{6}$$

The poloidal angle variable θ_* is obtained from the knowledge of the equilibrium magnetic field. The angle θ_* is related to θ through the periodic function $\lambda(\rho,\theta)$ by $\theta_* = \theta + \lambda(\rho,\theta)$. Here $\lambda(\rho,\theta)$ is the solution, for each ρ, of the differential equation

$$\frac{\partial\lambda}{\partial\theta} = \frac{\sqrt{g}B^3}{q(\rho)\psi'} - 1 , \tag{7}$$

where the right-hand-side (rhs) equilibrium quantities are expressed in terms of the ρ and θ coordinates.

The metric elements and their Fourier amplitudes in (ρ,θ_*,ϕ) coordinates can be constructed from their counterparts in the arbitrary (ρ,θ,ϕ) flux coordinate system. Explicit expressions for them are given in Appendix A.

III. MHD EQUILIBRIUM EQUATION

The equilibrium equation in rationalized mks units are

$$\nabla p = \mathbf{j}\times\mathbf{B} , \tag{8}$$

$$\mathbf{j} = \nabla\times\mathbf{B} . \tag{9}$$

In addition, the magnetic field $\mathbf{B}$ is divergence free, and ϕ is a coordinate of symmetry, so that the magnetic field is given by (1). The condition $\mathbf{B}\cdot\nabla p = 0$ implies that the pressure p depends on u_1 and u_2 only through ψ, so $p = p(\psi)$. The condition $(\nabla u_1 \times \nabla u_2)\cdot\nabla p = 0$ implies that the component of the magnetic field in the coordinate of symmetry in covariant representation, $B_3 = \sqrt{g}\mathbf{B}\cdot(\nabla u_1 \times \nabla u_2)$, is also a function of ψ alone, which we shall denote by $F(\psi)$. The equilibrium equation becomes a differential equation for the helical flux function ψ,

$$\nabla\cdot(K\nabla\psi) = -\frac{1}{h^2}\frac{dp}{d\psi} - KF\frac{dF}{d\psi} - 2K^2 hF , \tag{10}$$

where $K = [1 + h^2(X^2 + Y^2)]^{-1}$.

To solve this equation, the pressure, $p(\psi)$, and the longitudinal covariant component of the magnetic field, $F(\psi)$, as well as appropriate boundary conditions for ψ must be specified.

IV. APPROXIMATE ANALYTIC SOLUTION IN AN ELLIPTIC DOMAIN

An approximate solution of Eq. (10) may be obtained by means of an asymptotic expansion for a plasma equilibrium configuration with large aspect ratio. This type of solution has been previously developed for toroidal plasma equilibria.[10] Let us consider a plasma such that its boundary has an elliptic cross section. In rotating Cartesian coordinates, the plasma boundary is given by

$$(X - X_M)^2/a^2 + (Y^2/b^2) = 1 . \tag{11}$$

We choose the pressure profile to be $p(\psi) = P_\phi h^2(\psi_B^2 - \psi^2)/2a^2$, where ψ_B is the boundary value of the helical flux function. This choice ensures that the pressure vanishes at the boundary. The longitudinal component of the magnetic field is chosen as $F(\psi) = \beta_1\psi/a$. The parameters P_ϕ and β_1 are pure numbers. With this choice for p and F, the equilibrium equation (10) becomes a linear partial differential equation for ψ. Choosing the minor radius a as the unit of length, the equilibrium equation in rotating Cartesian coordinates, given our choice of p and F, is

$$\frac{\partial}{\partial X}[K\psi_X(1+\epsilon^2Y^2) - K\epsilon^2XY\psi_Y] + \frac{\partial}{\partial Y} \times [K\psi_Y(1+\epsilon^2X^2) - K\epsilon^2XY\psi_X] = (P_\phi - K\beta_1^2)\psi - 2K^2\epsilon\beta_1\psi , \tag{12}$$

where $K = [1 + \epsilon^2(X^2 + Y^2)]^{-1}$ and $\epsilon = ah = 2\pi(a/L)$. The boundary of the plasma in nondimensional form is given by $(X - X_M)^2 + (Y/E)^2 = 1$, where the ellipticity $E = (b/a)$. We now seek an asymptotic solution assuming that the inverse aspect ratio $\epsilon \ll 1$ and that P_ϕ and β_1 are of order one, but the difference $P_\phi - \beta_1^2$ is of order ϵ. Expanding ψ as a series in ϵ, $\psi = \psi_0 + \epsilon\psi_1 + \cdots$, we proceed to solve Eq. (12) to each order in ϵ. The solution for ψ is readily found, and it is given by

$$\psi = \psi_B\left(1 - \frac{\frac{1}{2}(P_\phi - \beta_1^2 - 2\epsilon\beta_1)(1-\rho^2)}{(1 - E^{-2})}\right) + O(\epsilon^2) . \tag{13}$$

We have introduced new variables ρ and θ through $X = X_M + \rho\cos\theta$, $Y = E\rho\sin\theta$. They constitute a magnetic flux coordinate system; ρ is the radial variable that varies between zero and one and labels flux surfaces, while θ is the poloidal angle variable that varies between 0 and 2π and sweeps along each flux surface. Here X_M is the distance from the magnetic axis to the geometric axis. The pressure profile turns out to be

$$p(\rho) = \frac{\frac{1}{2}P_\phi(h^2\psi_B/\epsilon)^2(P_\phi - \beta_1^2 - 2\epsilon\beta_1)(1-\rho^2)}{(1 + E^{-2})} + O(\epsilon^2) . \tag{14}$$

For this model equilibrium we may also compute the volume occupied by the plasma,

$$V = \int_0^{2\pi} d\phi \int_0^1 d\rho \int_0^{2\pi} d\theta\, \sqrt{g} , \tag{15a}$$

where $\sqrt{g}$ is the Jacobian of the transformation from (X, Y, Z) coordinates to (ρ, θ, ϕ) coordinates. The volume occupied by the plasma is

$$V = 2\pi^2 E\epsilon^2/h^3 . \tag{15b}$$

The plasma beta is the ratio of the volume-averaged pressure to the longitudinal field density,

$$\beta(\rho) = \frac{\langle p\rangle/V}{(B_0^2/2)} . \tag{16a}$$

In this model, with $B_0 = hF(\psi_B)$, we obtain

$$\beta = (P_\phi/2\beta_1^2)\left[(P_\phi - \beta_1^2 - 2\epsilon\beta_1)/(1+E^{-2})\right]. \tag{16b}$$

The plasma q value, which represents the inverse precession of a magnetic field line within a field period on a flux surface, is given by

$$q(\rho) = \frac{1}{2\pi}\frac{d}{d\psi}\left(\int\int(\mathbf{B}\cdot\nabla u_3)\sqrt{g}\,du_1\,du_2\right). \tag{17a}$$

In the magnetic flux coordinate system this is

$$q(\rho) = \frac{1}{2\pi}\frac{d}{d\psi}\left(\int_0^\rho d\rho\int_0^{2\pi} d\theta\,\sqrt{g}\right.$$
$$\left.\times\left[Kh^2F(\psi) - (Kh^2\psi'/\sqrt{g})(XY_\theta - YX_\theta)\right]\right),$$

which, up to order ϵ, in this model is

$$q(\rho) = \frac{\epsilon\beta_1 E(1+E^{-2})}{P_\phi - 2\epsilon\beta_1 - \beta_1^2} - \frac{1}{2}\beta_1\epsilon E(1-\rho^2). \tag{17b}$$

We notice that the ρ dependence of q is of order ϵ, so that the shear is small. At the outer edge, $\rho = 1$,

$$q = q_e = \epsilon\beta_1 E(1+E^{-2})(P_\phi - 2\epsilon\beta_1 - \beta_1^2)^{-1}.$$

On the axis, $\rho = 0$, $q = q_a = q_e - \frac{1}{2}\beta_1\epsilon E$. The longitudinal plasma current $I(\rho)$ is given by

$$I(\rho) = \int_0^\rho d\rho\int_0^{2\pi} d\theta\,\sqrt{g}(\mathbf{j}\cdot\nabla u_3), \tag{18a}$$

which, in this model, turns out to be a quantity of order ϵ:

$$I(\rho) = \pi hE\psi_B\rho^2\left((P_\phi - \beta_1^2) - \frac{1}{2}\frac{P_\phi - \beta_1^2 - 2\epsilon\beta_1}{1+E^{-2}}\right.$$
$$\times\left[(1-\tfrac{1}{2}\rho^2)(P_\phi - \beta_1^2) - \epsilon\beta_1\rho^2\right]$$
$$\left.+\beta_1^2\epsilon^2\left[X_M^2 + \tfrac{1}{4}(1+E^2)\rho^2\right]\right) + O(\epsilon^3). \tag{18b}$$

In this analytic solution of the MHD equilibrium equation, the free parameters $X_M, P_\phi, \beta_1, E, \epsilon, h$, and ψ_B may be specified arbitrarily. However, in generating sequences of equilibria with increasing P_ϕ, for example, a physically intuitive rather than an *ad hoc* choice for β_1 is desirable. There are two alternatives: (1) flux-conserving sequences and (2) zero longitudinal current sequences. Flux-conserving sequences identify equilibria in which the q profile is frozen while β is raised and are particularly suitable for modeling the rapid heating of a plasma to high temperatures. We can generate in this model approximate flux-conserving sequences by specifying q_e, q_a, ψ_B, h, X_M, P_ϕ, and the plasma volume V. The ellipticity E is then the greatest root of the quadratic equation

$$E^2[P_\phi - 2(q_e - q_a)/q_e] - 4(q_e - q_a)$$
$$\times[1 + [2\pi^2(q_e - q_a)/h^3V]]E - 2[(q_e - q_a)/q_e]$$
$$= 0,$$

which in leading order is $E = 8\pi^2(q_e - q_a)^2/(h^3VP_\phi)$; the parameter β_1 is given by $\beta_1 = 2(q_e - q_a)$ $\times(2\pi^2E/hV)^{1/2}/(hE)$, and $\epsilon = h(hV/2\pi^2E)^{1/2}$.

Alternatively, from Eq. (18b) we see that approximately zero longitudinal current sequences are obtained choosing $P_\phi = \beta_1^2$. The requirement that the plasma beta be positive implies that we must choose $\beta_1 = -\sqrt{P_\phi}$. The rest of the parameters remain free. In this case we distinguish two possibilities. We may fix the longitudinal magnetic field at the edge to a value F_e so that ψ_B varies from equilibrium to equilibrium according to $\psi_B = -\epsilon F_e/(h\sqrt{P_\phi})$, or we may fix ψ_B and let F_e vary. Finally, we notice that for this model equilibrium the periodic function $\lambda(\rho,\theta)$ obtained by integrating (7) is of order ϵ, so that $\cos\theta_* = \cos\theta + O(\epsilon)$ and $\sin\theta_* = \sin\theta + O(\epsilon)$.

The analytic equilibria we have described not only serve as a valuable benchmark for the numerical codes that are required to generate and investigate helically symmetric Heliac-type equilibria,[5] but also have useful applicability as models for the asperator[12] and the high beta Q-machine (HBQM)[13] devices.

Having obtained these analytic equilibria, we now proceed to investigate their stability to resistive ballooning modes.

V. THE RESISTIVE BALLOONING EQUATION IN SYSTEMS WITH A COORDINATE OF SYMMETRY

The MHD equations, linearized around an equilibrium pressure p and equilibrium magnetic field $\mathbf{B}$, are the momentum equation

$$\rho_M\frac{\partial\mathbf{v}}{\partial t} = -\nabla p_1 + (\nabla\times\mathbf{B}_1)\times\mathbf{B} + (\nabla\times\mathbf{B})\times\mathbf{B}_1, \tag{19}$$

the isothermal pressure evolution equation

$$\frac{\partial p_1}{\partial t} = -\mathbf{v}\cdot\nabla p, \tag{20}$$

Faraday's law

$$\frac{\partial\mathbf{B}_1}{\partial t} = -\nabla\times\mathbf{E}, \tag{21}$$

Ohm's law

$$\mathbf{E} + \mathbf{v}\times\mathbf{B}_1 = \eta(\nabla\times\mathbf{B}_1), \tag{22}$$

and Maxwell's second equation

$$\nabla\cdot\mathbf{B}_1 = 0. \tag{23}$$

Here ρ_M is the mass density, and η is the resistivity. A subscript 1 denotes a perturbation. The velocity $\mathbf{v}$ and electric field $\mathbf{E}$ are small. Letting any perturbation $\xi(\rho,\theta,\phi,t)$ be represented in its eikonal form[7]

$$\xi(\rho,\theta,\phi,t) = \hat{\xi}(\rho,\theta,t)e^{inS}, \tag{24}$$

with the mode number $n \gg 1$, we perform an expansion in $1/n$ of the linearized MHD equations [(19)–(23)]. In magnetic flux coordinates (ρ,θ,ϕ) the eikonal phase factor, which satisfies $\mathbf{B}\cdot\nabla S = 0$ and $\sqrt{g}\,\nabla\rho\times\nabla\theta\cdot\nabla S = 1$, is given by

$$S = \phi - \int_0^\theta d\theta(\sqrt{g}B^3/\psi') + k_v(\rho), \tag{25a}$$

or, in the straight field line coordinate system,

$$S = \phi - q\theta_* + k_v(\rho), \tag{25b}$$

where k_v, the radial wavenumber, is an arbitrary function of ρ.

In performing the expression of the MHD equations in

powers of $1/n$, it is convenient to expand the perturbation to the magnetic field $\mathbf{B}_1$ and the velocity $\mathbf{v}$ into components that are along the magnetic field lines, normal to the flux surfaces (radial), and binormal, namely

$$\mathbf{B}_1 = \hat{b}(\mathbf{B}_1 \cdot \hat{b}) + \nabla\rho \frac{\mathbf{B}_1 \cdot \nabla\rho}{|\nabla\rho|^2} + \hat{b} \times \nabla\rho \frac{\mathbf{B}_1 \cdot \hat{b} \times \nabla\rho}{|\nabla\rho|^2},$$

$$\mathbf{v} = \hat{b}(\mathbf{v} \cdot \hat{b}) + \nabla\rho \frac{\mathbf{v} \cdot \nabla\rho}{|\nabla\rho|^2} + \hat{b} \times \nabla\rho \frac{\mathbf{v} \cdot \hat{b} \times \nabla\rho}{|\nabla\rho|^2},$$

where

$$\hat{b} = \mathbf{B}/|\mathbf{B}| .$$

Now we perform an asymptotic expansion for all the perturbations $\hat{\xi}(\rho, \theta, t) = \hat{\xi}^{(0)} + (1/n)\hat{\xi}^{(1)} + \ldots$. Evaluating the condition $\nabla \cdot \mathbf{B}_1 = 0$, we find that there is a relation between the order $(1/n)^0$ components of the radial and binormal perturbed magnetic fields given by

$$\mathbf{B}_1^{(0)} \cdot (\hat{b} \times \nabla\rho) = + \left(\frac{d\psi}{d\rho}\right) \frac{\nabla\rho \cdot \nabla S}{|\mathbf{B}|} [\mathbf{B}_1^{(0)} \cdot \nabla\rho] . \tag{26}$$

The combination of Faraday's law and Ohm's law yields the equation

$$\frac{\partial \mathbf{B}_1}{\partial t} = - \nabla \times [\eta(\nabla \times \mathbf{B}_1)] + \nabla \times (\mathbf{v} \times \mathbf{B}) . \tag{27}$$

Ignoring the spatial variations of the resistivity, since we wish to neglect the effect of rippling modes, Eq. (27) becomes

$$\frac{\partial \mathbf{B}_1^{(0)}}{\partial t} = - (n^2\eta)|\nabla S|^2 \mathbf{B}_1^{(0)} + \nabla \times (\mathbf{v}^{(0)} \times \mathbf{B}) , \tag{28}$$

where we assume that $n^2\eta$ is a quantity of order 1. The leading order component of Ohm's law along a magnetic field line implies that $\nabla \cdot \mathbf{v}$ is a quantity of order 1. Evaluating $\nabla \cdot \mathbf{v}$, we find that to satisfy this condition, the factors that are of order 1 must vanish. This yields a relation between the leading order components of the binormal and radial velocities analogous to Eq. (26), namely,

$$\mathbf{v}^{(0)} \cdot \hat{b} \times \nabla\rho = \left(\frac{d\psi}{d\rho}\right) \frac{\nabla\rho \cdot \nabla S}{B} (\mathbf{v}^{(0)} \cdot \nabla\rho) . \tag{29}$$

The radial component of Ohm's law is

$$\frac{\partial}{\partial t}(\mathbf{B}_1^{(0)} \cdot \nabla\rho) = - n^2\eta|\nabla S|^2 (\mathbf{B}_1^{(0)} \cdot \nabla\rho) + (\mathbf{B} \cdot \nabla)(\mathbf{v}^{(0)} \cdot \nabla\rho) . \tag{30}$$

The evaluation of the binormal component of the equation of motion shows that

$$\hat{p}_1^{(0)} + \mathbf{B} \cdot \mathbf{B}_1^{(0)} = 0 , \tag{31}$$

$$\hat{p}_1^{(1)} + \mathbf{B} \cdot \mathbf{B}_1^{(1)} = \frac{1}{iB}\left(\frac{d\psi}{d\rho}\right)\left(\rho_M \frac{\partial}{\partial t}(\hat{b} \times \nabla\rho \cdot \mathbf{v}^{(0)}) - (\mathbf{B} \cdot \nabla) \times (\hat{b} \times \nabla\rho \cdot \mathbf{B}_1^{(0)}) - \mathbf{B}_1^{(0)} \cdot [\nabla\rho(\hat{b} \cdot \nabla \times \mathbf{B}) + \nabla\rho \times \nabla B + \hat{b}(\hat{b} \cdot \nabla\rho \times \nabla B)]\right) . \tag{32}$$

Expanding ∇S in radial and binormal components, one can show that

$$\left[1 + \left(\frac{d\psi}{d\rho}\right)^2 \left(\frac{\nabla\rho \cdot \nabla S}{B}\right)^2\right] = \left(\frac{d\psi}{d\rho}\right)^2 (\nabla\rho)^2 \frac{(\nabla S)^2}{B^2} . \tag{33}$$

Then we can express

$$B(\mathbf{K} \cdot \nabla\rho) + \frac{d\psi}{d\rho} \frac{\nabla\rho \cdot \nabla S}{B} \hat{b} \times \nabla\rho \cdot \nabla B = \frac{d\psi}{d\rho}(\nabla\rho)^2 (\hat{b} \times \nabla S \cdot \mathbf{K}) , \tag{34}$$

where $\mathbf{K} = (\hat{b} \cdot \nabla)\hat{b}$ is the magnetic field line curvature, and after some algebraic manipulations the leading order radial equation becomes

$$\rho_M \frac{(\nabla S)^2}{B^2} \frac{\partial}{\partial t}(\mathbf{v}^{(0)} \cdot \nabla\rho) = (\mathbf{B} \cdot \nabla)\left(\frac{(\nabla S)^2}{B^2} [\mathbf{B}_1^{(0)} \cdot \nabla\rho]\right) - \frac{2}{B(d\psi/d\rho)} (\hat{b} \times \nabla S \cdot \mathbf{K}) \hat{p}_1^{(0)} \tag{35}$$

The initial value resistive ballooning-mode equations for systems having a coordinate of symmetry are Eqs. (30), (35), and the isothermal pressure evolution equation, which in leading order is

$$\frac{\partial \hat{p}_1^{(0)}}{\partial t} = - \frac{dp}{d\rho} (\mathbf{v}^{(0)} \cdot \nabla\rho) , \tag{36}$$

since the equilibrium pressure is only a function of ρ.

So the resistive initial value ballooning equations consist of three partial differential equations, with the radial velocity, radial magnetic field, and pressure perturbations advanced in time. Finally, assuming that the perturbations evolve as $e^{\gamma t}$, the initial value equations can be combined into a single ordinary differential equation for the radial velocity perturbation along the magnetic field lines of each flux surface, that is,

$$(\mathbf{B} \cdot \nabla)\left(\frac{(\nabla S)^2}{B^2} \frac{(\mathbf{B} \cdot \nabla)(\mathbf{v}^{(0)} \cdot \nabla\rho)}{[1 + (n^2\eta/\gamma)(\nabla S)^2]}\right) + \frac{2}{B^2} \frac{dp}{d\psi} \times (\mathbf{B} \times \nabla S \cdot \mathbf{K})(\mathbf{v}^{(0)} \cdot \nabla\rho) - \rho_M \gamma^2 \frac{(\nabla S)^2}{B^2} (\mathbf{v}^{(0)} \cdot \nabla\rho) = 0 . \tag{37}$$

The first term in this equation represents the field line bending, which has a stabilizing effect; the second term represents the interaction between the pressure gradient and the magnetic field line curvature that drives ballooning and interchange modes; and the third term represents the inertia. We notice that resistivity weakens the effect of the stabilizing field line bending term. Scaling the longitudinal magnetic field F by its value at the edge F_e, the helical flux function by $\epsilon^2 F_e/h$, the Jacobian by ϵ^2/h^3, the upper metric elements by h^2/ϵ^2, the pressure by p_0 (its value on the axis), the growth rate γ by the poloidal Alfvén frequency $\gamma_0 = h^2 F_e/\sqrt{\rho_M}$, and the resistivity by its value η_0 on the axis, the resistive ballooning-mode equation in the straight field line magnetic flux coordinate system (ρ, θ_*, ϕ) becomes[11]

$$\frac{\partial}{\partial\theta_*}\left(\frac{(\nabla S)^2\psi'}{\sqrt{g}B^2[1+(n^2/S_R)(\eta/\gamma)(\nabla S)^2]}\frac{\partial v_\rho}{\partial\theta_*}\right)$$
$$+\frac{\beta_0}{\epsilon^2}\left(\frac{\sqrt{g}}{\psi'B^2}\frac{dp}{d\psi}(\mathbf{B}\times\nabla S\cdot\mathbf{K})v_\rho\right)-\frac{\sqrt{g}}{\psi'}\gamma^2\frac{(\nabla S)^2}{B^2}v_\rho$$
$$=0\,, \tag{38}$$

where

$$B^2=(\psi')^2[g^{\rho\rho}(g^{\phi\phi}-2qg^{\phi\theta_*}+q^2g^{\theta_*\theta_*})$$
$$-(g^{\rho\phi}-qg^{\rho\theta_*})^2]\,,$$
$$(\nabla S)^2=g^{\phi\phi}-qg^{\phi\theta_*}-q(g^{\phi\theta_*}-qg^{\theta_*\theta_*})$$
$$-2q'(g^{\phi\rho}-qg^{\rho\theta_*})(\theta_*-\theta_k)$$
$$+(q')^2g^{\rho\rho}(\theta_*-\theta_k)^2\,,$$
$$\mathbf{B}\times\nabla S\cdot\mathbf{K}=\frac{1}{2\psi'}\frac{\partial}{\partial\rho}(\beta_0p'+B^2)-\frac{1}{2B^2}\frac{\partial B^2}{\partial\theta_*}\left(\frac{F}{\sqrt{g}}q'\right.$$
$$\times(\theta_*-\theta_k)+\psi'g^{\rho\phi}(g^{\theta_*\phi}-qg^{\theta_*\theta_*})$$
$$\left.-\psi'g^{\rho\theta_*}(g^{\phi\phi}-qg^{\theta_*\phi})\right).$$

Here, $\theta_k=dk_v/dq$ and $v_\rho=\mathbf{v}^{(0)}\cdot\nabla\rho$. With this scaling, the nondimensional parameters that appear in the equation are $\epsilon=ah$, the magnetic Reynolds number $S_R=a^2\gamma_0/\eta_0$, the mode number n, and $\beta_0=2\,p_0/h^2F_e^2$. We have solved this equation numerically to test the stability of the equilibria described in Sec. IV.

VI. REDUCED RESISTIVE BALLOONING EQUATION

The coefficients that appear in the ballooning-mode equation (38) adopt a particularly simple form if we assume that the equilibrium configuration has a large aspect ratio. This is, in fact, the case we deal with when we study the equilibria described in Sec. IV. Thus we perform an expansion of Eq. (38) in the small parameter $\epsilon=ah$ to obtain a reduced resistive ballooning equation. In what follows, the subscript * has been dropped from the variable θ; nonetheless, we are still dealing with that coordinate system. We first consider the stabilizing field line bending and inertia. An asymptotic expansion shows that to leading order

$$\sqrt{g}=q(\psi'/F)+O(\epsilon^2)\,, \tag{39}$$
$$B^2=F^2+O(\epsilon^2)\,, \tag{40}$$
$$(\nabla S)^2=(F/\psi')^2\alpha_\perp\,, \tag{41}$$

where

$$\alpha_\perp=X_\rho^2+Y_\rho^2-2(q'/q)(X_\rho X_\theta+Y_\rho Y_\theta)(\theta-\theta_k)$$
$$+(q'/q)^2(X_\theta^2+Y_\theta^2)(\theta-\theta_k)^2\,. \tag{42}$$

In order to obtain the leading order expansion of the destabilizing term, one can show that

$$\mathbf{B}\times\nabla S\cdot\mathbf{K}$$
$$=\frac{1}{2\psi'}\frac{\partial}{\partial\rho}(\beta_0p+B^2)+\frac{1}{2B^2}\frac{\partial B^2}{\partial\theta}(\mathbf{B}\times\nabla S\cdot\nabla\theta)\,, \tag{43}$$

$$\mathbf{B}\times\nabla S\cdot\nabla\theta$$
$$=-\frac{q'}{\sqrt{g}}F(\theta-\theta_k)-\epsilon^2\frac{\psi'}{g}(g_{\rho\theta}+qg_{\rho\phi})\,. \tag{44}$$

Now, in leading order, one can show that

$$\frac{\partial B^2}{\partial\theta}=2(\epsilon F)^2\frac{1}{qq'}K_S\,, \tag{45}$$

where the function $K_S(\rho,\theta)$, given by

$$K_S=-(q'/q)[q^2(XX_\theta+YY_\theta)-X_\theta X_{\theta\theta}-Y_\theta Y_{\theta\theta}]\,, \tag{46}$$

is related to the geodesic curvature. We also have

$$\frac{\partial B^2}{\partial\rho}=2FF'-2\epsilon^2F^2\left[XX_\rho+YY_\rho-\frac{1}{q^2}\right.$$
$$\times(X_\theta X_{\rho\theta}+Y_\theta Y_{\rho\theta})+\frac{q'}{q^3}(X_\theta^2+Y_\theta^2)$$
$$\left.+\frac{F'}{F}\left(X^2+Y^2-\frac{1}{q^2}(X_\theta^2+Y_\theta^2)\right)\right]+O(\epsilon^4)\,. \tag{47}$$

An expansion of the equilibrium equation (10), properly normalized, shows that

$$\frac{1}{2}(\beta_0p'+2FF')=-\left(\frac{\epsilon F}{q}\right)^2\left[-q^2\frac{F'}{F}(X^2+Y^2)\right.$$
$$+\left(\frac{F'}{F}-\frac{q'}{q}\right)(X_\theta^2+Y_\theta^2)+X_\theta X_{\rho\theta}+Y_\theta Y_{\rho\theta}$$
$$\left.-X_\rho X_{\theta\theta}-Y_\rho Y_{\theta\theta}+2q(X_\rho Y_\theta-Y_\rho X_\theta)\right]+O(\epsilon^4)\,, \tag{48}$$

and so we have

$$\frac{\partial}{\partial\rho}(\beta_0p+B^2)=-2\left(\frac{\epsilon F}{q}\right)^2K_p(\rho,\theta)+O(\epsilon^4)\,, \tag{49}$$

where the function $K_p(\rho,\theta)$, given by

$$K_p=q^2(XX_\rho+YY_\rho)+2q(X_\rho Y_\theta-Y_\rho X_\theta)$$
$$-(X_\rho X_{\theta\theta}+Y_\rho Y_{\theta\theta})\,, \tag{50}$$

is related to the normal curvature.

Combining the expressions above we find that

$$\mathbf{B}\times\nabla S\cdot\mathbf{K}=-(\epsilon F/q)^2(1/\psi')[K_p+K_S(\theta-\theta_k)]\,, \tag{51}$$

in such a way that the reduced resistive ballooning equation, to leading order, becomes

$$\frac{\partial}{\partial\theta}\left[\left(\left(\frac{F}{\psi'}\right)^2\alpha_\perp\frac{\partial v_\rho}{\partial\theta}\right)\left(1+\frac{n^2}{S_R}\frac{\eta}{\gamma}\frac{F^2}{(\psi')^2}\alpha_\perp\right)^{-1}\right]$$
$$-\left(\frac{\gamma q}{\psi'}\right)^2\alpha_\perp v_\rho-\frac{\beta_0p'}{(\psi')^2}[K_p+K_S(\theta-\theta_k)]v_\rho$$
$$=0\,. \tag{52}$$

VII. ANALYTIC GROWTH RATE SCALING

The reduced ballooning equation (52) may be solved approximately and an analytic expression for the growth rate γ be found using a two-length scale expansion[14] for the model equilibria described in Sec. IV, which consist of a plasma with elliptical flux surfaces represented by

$$X = X_M + \rho\cos\theta, \quad Y = E\rho\sin\theta .$$

The equilibrium quantities in Eq. (52) are

$$\alpha_\perp = \tfrac{1}{2}(E^2+1)[1+s^2(\theta-\theta_k)^2] - (E^2-1)(\theta-\theta_k)s\sin(2\theta) + \cos 2\theta\,[(1-E^2)/2][1-s^2(\theta-\theta_k)^2], \tag{53}$$

$$K_p = 2(\psi' q^2/F) + \rho(1+q^2)\tfrac{1}{2}(1+E^2) + q^2 X_M\cos\theta + \tfrac{1}{2}\rho(1+q^2)(1-E^2)\cos(2\theta), \tag{54}$$

$$K_S = sq^2 X_M\sin\theta - \rho s[(E^2-1)/2](1+q^2)\sin(2\theta), \tag{55}$$

where $s \equiv \rho q'/q$ is the shear parameter. If we now invoke the electrostatic approximation, which is valid for large $(\theta-\theta_k)$, the reduced ballooning resistive equation for the model equilibria becomes

$$a_r\gamma\frac{\partial^2 v_\rho}{\partial\theta^2} = [A_1(\theta) + A_2(\theta)\sin\theta + A_3(\theta)\cos\theta + A_4(\theta)\sin 2\theta + A_5(\theta)\cos 2\theta]v_\rho . \tag{56}$$

The coefficients $A_i(\theta)$, $i = 1,\ldots, 5$ are given in Appendix B. We have defined $a_r = S_R/n^2\eta$.

Equation (56) may be solved approximately, assuming that v_ρ has a two-length scale expansion of the form

$$v_\rho = V_0 + V_s\sin\theta + V_c\cos\theta + W_s\sin(2\theta) + W_c\cos(2\theta),$$

where V_0, V_s, V_c, W_s, and W_c are slowly varying amplitudes. We find expressions for V_s, V_c, W_s, W_c in terms of V_0, and then we find the evolution equation for V_0. The lengthy expressions involved are given in Appendix B. Finally, we consider the large $(\theta-\theta_k)$ behavior of this equation to obtain a potential equation of the form,

$$\frac{d^2V_0}{d\chi^2} + (C_1 - C_2\chi^2)V_0 = 0, \tag{57}$$

where the coefficients C_1 and C_2 are given in Appendix B, and $\chi = s(\theta-\theta_k)$. The solution to Eq. (57) is an envelope $\exp[-\chi^2/2L^2]$, with the width of the mode L given by

$$L = \left(\frac{2a_r(\psi')^2}{\gamma s\, q^2(1+E^2)}\right)^{1/4}\left[1-\frac{1}{2}\left(\frac{1-E^2}{1+E^2}\right)\right]^{-1/4}. \tag{58}$$

In the regime dominated by the resistive ballooning mode, which corresponds to

$$\gamma \ll [2(\psi')^2 a_r/q^2][g_2(E)/g_4(E)],$$

$$\gamma \gg \frac{1}{2a_r}\frac{\beta_0 p'}{(\psi')^2}\left(\rho(1+q^2)\frac{g_4(E)}{g_2(E)} + 2\frac{\psi' q^2}{F}\frac{g_5(E)}{g_2(E)}\right),$$

we obtain the growth rate

$$\gamma = (n^2\eta/S_R)^{1/3}(\beta_0 p' q/2\psi')^{2/3}(f_1(E)X_M^2 + f_2(E)\{\rho[(1+q^2)/q^2]\}^2)^{1/3}. \tag{59}$$

The functions of the ellipticity $g_i(E)$ and $f_i(E)$ are given in Appendix B. The first term on the rhs of Eq. (59) corresponds to the interaction of the pressure gradient with the magnetic field line curvature induced by the helical nature of the magnetic axis, which we have identified as a ballooning-mode driving mechanism.[15] The second term on the rhs represents the interaction of the pressure gradient with the component of the curvature induced by the elliptic distortion of a flux surface away from a circle. This term corresponds to an additional source of energy to drive ballooning modes. It vanishes in the limit that the flux surfaces are circular.

VIII. NUMERICAL RESULTS

The ballooning-mode equation (38) and the reduced equation (52) have been integrated numerically using a shooting method. We have studied the stability of the approximate analytic equilibria described in Sec. V. We assume a resistivity profile given by Spitzer's law $\eta \sim p^{-3/2}$. In order to compare different equilibria, a base case has been fixed with respect to which the rest are normalized. Thus for flux-conserving equilibria, the magnetic Reynolds number S_R is given by $S_R = S_{Rb}(a/a_b)^2(\beta_0/\beta_{0b})^{3/2}$. The subscript "$b$" denotes the values for the base case. For approximate zero longitudinal current equilibria, if the longitudinal magnetic field F is fixed on the edge, then $S_R = S_{Rb}(\beta_0/\beta_{0b})^{3/2}$ and, if the helical flux function ψ is given on the edge, then

$$S_R = S_{Rb}(F_e/F_{eb})^4(\beta_0/\beta_{0b})^{3/2}.$$

The growth rates obtained from integrating Eqs. (38) and (52) are compared with the values obtained from the approximate analytic dispersion relation, Eq. (59).

The model equilibria under consideration have low shear, and therefore both the unstable ideal and resistive ballooning modes are very extended in the poloidal angle variable. To obtain the dispersion relation, we have invoked the electrostatic approximation which eliminates the ideal instabilities and is valid at large θ. The purely resistive ballooning modes remain. We expect, then, that the scaling obtained from the full ballooning-mode equation is very similar to that obtained from the dispersion relation with an offset resulting from the residual ideal mode.

The basic equilibrium with respect to which we normalize has $P_\phi = 0.3$, plasma volume $V = 947.48$, $\psi_B = 0.6$, ellipticity $E = 1.6$, $X_M = 1.0$, $q_a = -1.0979$, $q_e = -1.1125$, $h = \frac{1}{30}$, $\epsilon = \frac{1}{30}$, and $F_e = -0.3286335$. This yields $\beta_0 = 0.02608549$. We also take $S_{Rb} = 10^4$ and a basic mode number $n = 70$. In all cases we take 50 points on each magnetic surface and six modes to reconstruct the geometric quantities needed on each flux surface.

In Fig. 1, we compare the eigenfunctions obtained from the full and reduced equations for different mode numbers. They agree quite well. As has already been pointed out,[16] as n increases, the mode extends less in θ to overcome the influence of the field line bending term. Thus, the mode is less radially localized in real space.

For the two kinds of equilibria considered, we have studied the effect of varying the mode number n, the ellipticity E, the plasma β, and the distance X_M from the magnetic axis to the geometric axis. The results are shown in Figs. 2–9 for a point midway between the center and the plasma edge, namely $\rho = 0.547$. In all cases we find reasonable agreement

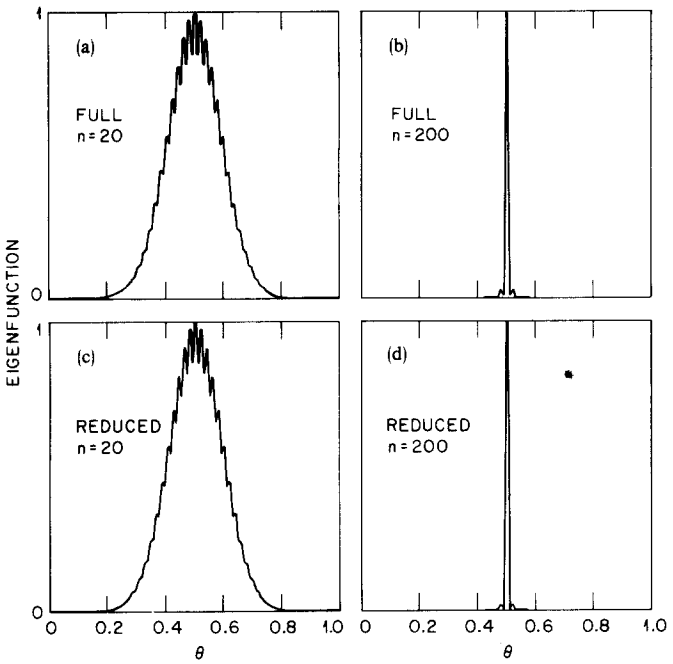

FIG. 1. The eigenfunction structures from the full and the reduced ballooning-mode equations for different values of n: (a) full equation, $n = 20$, (b) full equation, $n = 200$, (c) reduced equation, $n = 20$, and (d) reduced equation, $n = 200$. The domain of integration is $-51\pi < \theta < 51\pi$, and the magnetic Reynolds number is $S_R = 1.24 \times 10^4$.

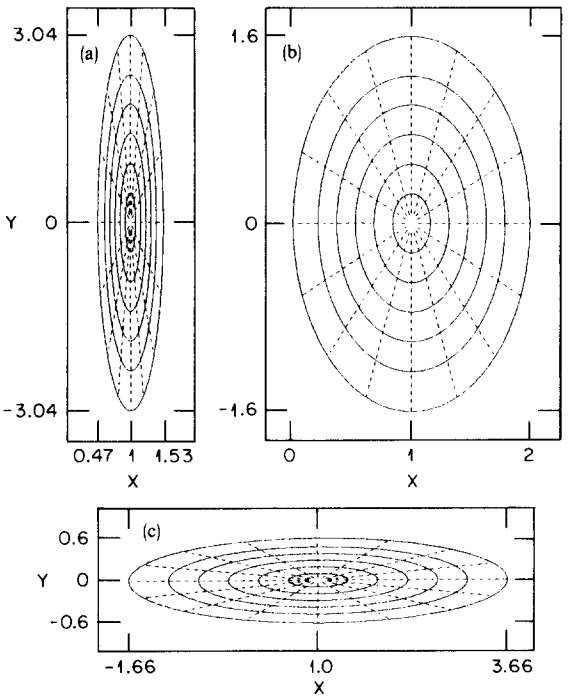

FIG. 3. Cross sections of the flux surfaces for a flux-conserving equilibrium sequence with fixed plasma volume. The base case is configuration (b). Case (a) is obtained by decreasing P_ϕ, and case (c) is obtained by increasing P_ϕ.

between the growth rates obtained from the numerical integration of the full and the reduced resistive ballooning equations. The growth rates obtained from the dispersion relation reproduce the scaling obtained from the full equation with an offset that corresponds to the fact explained above. The solution of the full ballooning mode equation [Eq. (38)] as a function of β for three different sequences of equilibria is presented in Fig. 2. The base case corresponds to the intersection of the three curves at $\beta \simeq 1.3\%$. The zero longitudinal current curve labeled option 1 corresponds to the sequence for which ψ_B, the helical magnetic flux at the plasma boundary, remains fixed, and that labeled option 2 corresponds to the sequence for which F_e, the longitudinal magnetic field (in covariant representation) at the edge of the plasma, remains fixed. For both these sequences, the smaller values of β are obtained by decreasing the parameter P_ϕ, and the higher values of β are obtained by increasing P_ϕ. The plasma volume and the ellipticity are also fixed for these cases. Starting at the base case, if we decrease P_ϕ in the flux-conserving sequence, the plasma β actually increases and yields the branch with the smaller growth rates in Fig. 2. If we increase P_ϕ, the plasma β decreases slightly at first and then increases to yield the branch with the higher growth rates. This effect is a result of the fact that the ellipticity is

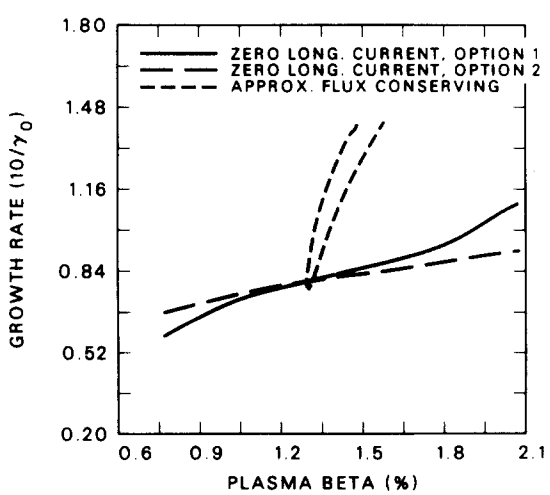

FIG. 2. The growth rates in units of $0.1\ \gamma_0$ as a function of β from the full ballooning-mode equation for a flux-conserving equilibrium sequence, a zero current equilibrium sequence with ψ_B constant (option 1), and zero current equilibrium sequence with F_e constant (option 2).

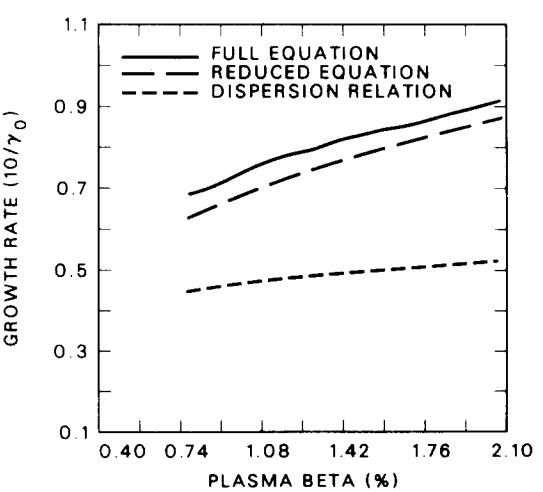

FIG. 4. The resistive ballooning-mode growth rates in units of $0.1\gamma_0$ as a function of β from the full equation, the reduced equation, and the dispersion relation for the zero current equilibrium sequence with constant F_e.

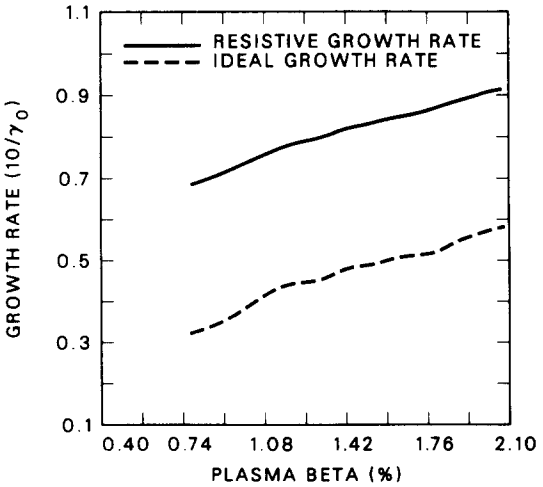

FIG. 5. The resistive and ideal ballooning-mode growth rates in units of $0.1\gamma_0$ as a function of β from the full equation for the zero current equilibrium sequence with constant F_e.

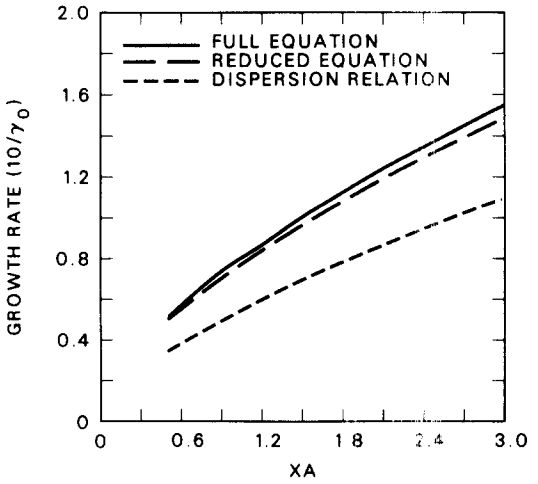

FIG. 7. The resistive ballooning-mode growth rates in units of $0.1\gamma_0$ as a function of $XA = X_M$, the distance between the magnetic axis and the geometric axis, from the full equation, the reduced equation, and the dispersion relation.

variable in the flux-conserving sequence and has an impact on the value of β. This variation in the plasma shape is demonstrated in Fig. 3. The base case, which has ellipticity $E = 1.6$, corresponds to the configuration labeled (b) in Fig. 3. Decreasing P_ϕ yields the more elliptical configuration that we label (a), and increasing P_ϕ yields the configuration with prolate ellipticity ($E < 1$) labeled (c).

In Fig. 4, we compare the resistive ballooning-mode growth rates as a function of β for the zero current sequence with constant F_e from the full ballooning-mode equation [Eq. (38)], the reduced ballooning-mode equation [Eq. (52)], and the dispersion relation [Eq. (59)]. The divergence between the numerical solutions and the dispersion relation with increasing β is attributable to the increase of the ideal growth rate which becomes evident by examining Fig. 5. We have also carried out a comparison analogous to that shown in Fig. 4 for the flux-conserving equilibrium sequence, and the results are presented in Fig. 6. The resistive ballooning-mode growth rates predicted by the full equation, the reduced equation, and the dispersion relation are displayed as functions of X_M and E, respectively, in Figs. 7 and 8. The curvature effects induced by the helical magnetic axis and the effects of ellipticity, either prolate or oblate, are destabilizing. Finally, in Fig. 9, we present the dependence of the growth rates on the mode number from the full equation and the dispersion relation. The growth rates scale as $n^{2/3}$. However, as n increases the mode structure becomes finer and finite Larmor radius effects, which are neglected in the resistive MHD model, become important.

IX. CONCLUSION

We have studied the resistive ballooning stability of helically symmetric equilibria. For the purpose of completeness we have rederived the MHD equilibrium equation and ballooning-mode equations. We have solved the equilibrium equation by means of an asymptotic expansion for large-aspect-ratio configurations. Thus, we obtain analytic expressions for flux-conserving and for zero-longitudinal-current equilibria of elliptical cross section. The stability of these

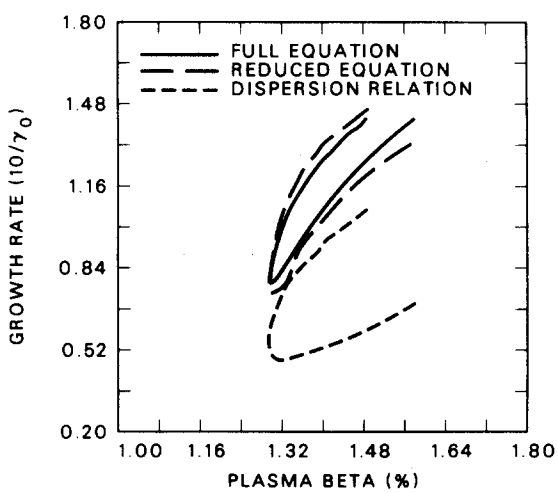

FIG. 6. The resistive ballooning-mode growth rates in units of $0.1\gamma_0$ as a function of β from the full equation, the reduced equation, and the dispersion relation for the flux-conserving equilibrium sequence.

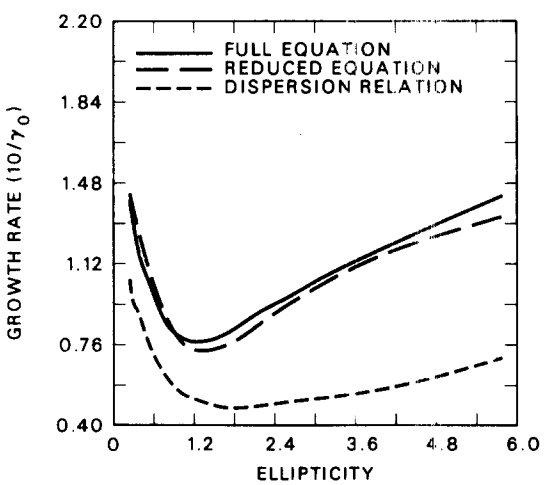

FIG. 8. The resistive ballooning-mode growth rates in units of $0.1\gamma_0$ as a function of the ellipticity from the full equation, the reduced equation, and the dispersion relation.

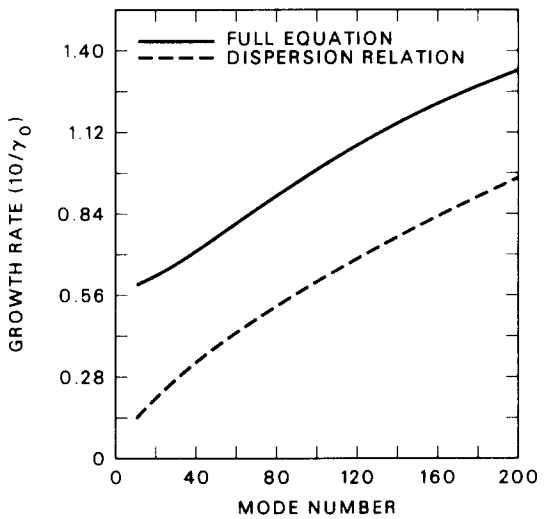

FIG. 9. The resistive ballooning-mode growth rates in units of $0.1\gamma_0$ as a function of the longitudinal mode number from the full equation and the dispersion relation.

equilibria with respect to resistive ballooning-mode instability is studied numerically. Analytic progress is possible because of our constraint to large-aspect-ratio systems, which enables us to obtain a simpler equation. The results obtained from the numerical integration of the full and reduced equation are in good agreement. Finally, we perform a two-scale expansion of the reduced equation. In the electrostatic approximation, valid for large $(\theta - \theta_k)$, we are able to find an analytic expression for the growth rate which shows that the instability arises from the interaction of the pressure gradient with the magnetic field line curvature. We find that two effects are present; in the first place there is the curvature induced by the helical nature of the magnetic axis, but also there is an effect resulting from the curvature induced by the elliptic distortion of the flux surfaces away from a circle. The comparison of the growth rates obtained from the numerical integration of the full equation and the approximate analytic growth rate shows that the scaling obtained is correct but that there is an offset resulting from the residual ideal modes.

The importance of investigating resistive ballooning modes is the link that has been established between them and the deterioration of confinement at relatively modest values of β in tokamaks.[17] Because these modes are driven by gradients in the pressure, similar effects should be expected in stellarator configurations also. In this article, we have investigated the resistive ballooning modes in a stellarator with a helical magnetic axis and have found that they scale as $\eta^{1/3}$. It is of value to note that the resistive interchange mode,[18,19] which is a different type of pressure-driven instability, also obeys the $\eta^{1/3}$ scaling that we have derived for the resistive ballooning mode.

ACKNOWLEDGMENTS

Research sponsored by the Dirección de Investigación, U. Católica de Chile, through DIUC Project No. 19/85 and by the Office of Fusion Energy, U. S. Department of Energy, under Contract No. DE-AC05-84OR21400 with Martin Marietta Energy Systems, Inc.

APPENDIX A: METRIC ELEMENT TRANSFORMATION TO STRAIGHT FIELD LINE COORDINATES

The upper metric elements $g_{ij} = \nabla u_i \cdot \nabla u_j$ are given by

$$g^{\rho\rho} = \frac{(1+h^2Y^2)Y_\theta^2 + 2h^2XYX_\theta Y_\theta + (1+h^2X^2)X_\theta^2}{(h^2 g)},$$

$$g^{\rho\theta} = -[(1+h^2Y^2)Y_\rho Y_\theta + (1+h^2X^2)X_\rho X_\theta + h^2XY(X_\rho Y_\theta + X_\theta Y_\rho)]/(h^2 g),$$

$$g^{\rho\phi} = h(XX_\theta + YY_\theta)/\sqrt{g},$$

$$g^{\theta\theta} = \frac{(1+h^2X^2)X_\rho^2 + (1+h^2Y^2)Y_\rho^2 + 2h^2XYX_\rho Y_\rho}{(h^2 g)},$$

$$g^{\theta\phi} = -h(XX_\rho + YY_\rho)/\sqrt{g}, \quad g^{\phi\phi} = h^2,$$

and the lower metric elements g_{ij} are given by

$$g_{\rho\rho} = X_\rho^2 + Y_\rho^2, \quad g_{\rho\theta} = X_\rho X_\theta + Y_\rho Y_\theta,$$

$$g_{\theta\theta} = X_\theta^2 + Y_\theta^2, \quad g_{\rho\phi} = XY_\rho - YX_\rho,$$

$$g_{\phi\phi} = [1 + h^2(X^2 + Y^2)]/h^2,$$

$$g_{\theta\phi} = XY_\theta - YX_\theta.$$

The upper metric elements in the straight field line coordinate system are obtained by noting that

$$\nabla\theta_* = \left(1 + \frac{\partial\lambda}{\partial\theta}\right)\nabla\theta + \frac{\partial\lambda}{\partial\rho}\nabla\rho.$$

Hence we get

$$g^{\rho\theta_*} = \left(1 + \frac{\partial\lambda}{\partial\theta}\right)g^{\rho\theta} + \frac{\partial\lambda}{\partial\rho}g^{\rho\rho},$$

$$g^{\theta_*\theta_*} = \left(1 + \frac{\partial\lambda}{\partial\theta}\right)^2 g^{\theta\theta} + 2\frac{\partial\lambda}{\partial\rho}\left(1 + \frac{\partial\lambda}{\partial\theta}\right)g^{\rho\theta} + \left(\frac{\partial\lambda}{\partial\rho}\right)^2 g^{\rho\rho},$$

$$g^{\theta_*\phi} = \left(1 + \frac{\partial\lambda}{\partial\theta}\right)g^{\theta\phi} + \frac{\partial\lambda}{\partial\rho}g^{\rho\phi},$$

while the rest of the upper metric elements remain unchanged. The lower metric elements keep the same expression, but this time the derivatives are referred to the new variables. In order to construct the Fourier amplitudes of the upper metric elements in the (ρ, θ_*, ϕ) coordinate system, we note that the upper metric elements in the (ρ, θ, ϕ) coordinates have definite parity; in fact, $g^{\rho\rho}$, $g^{\theta\theta}$, $g^{\phi\phi}$, and $g^{\theta\phi}$ as well as $\sqrt{g}$ are even functions of θ, while $g^{\rho\theta}$ and $g^{\rho\phi}$ are odd functions of θ. Furthermore, the contravariant longitudinal magnetic field B^3 is given by

$$B^3 = \frac{F - \sqrt{g}(d\psi/d\rho)(g^{\rho\phi}g^{\rho\theta} - g^{\theta\phi}g^{\rho\rho})}{g[g^{\rho\rho}g^{\theta\theta} - (g^{\rho\theta})^2]},$$

which is an even function of θ. Therefore, $\lambda(\rho,\theta)$ is an odd function of θ. This in turn implies that the upper metric elements $g^{\theta_*\theta_*}$ and $g^{\theta_*\phi}$ are even, while $g^{\rho\theta_*}$ is odd. Their Fourier amplitudes are thus given by

$$(g^{\rho\theta_*})_m = \frac{1}{\pi}\int_0^{2\pi} d\theta\left(1 + \frac{\partial\lambda}{\partial\theta}\right)\sin[m(\lambda+\theta)]g^{\rho\theta_*},$$

$$(g^{\theta_*\theta_*})_m = \frac{1}{\pi}\int_0^{2\pi} d\theta\left(1 + \frac{\partial\lambda}{\partial\theta}\right)\cos[m(\lambda+\theta)]g^{\theta_*\theta_*} - \frac{1}{2\pi}\int_0^{2\pi} d\theta\left(1 + \frac{\partial\lambda}{\partial\theta}\right)g^{\theta_*\theta_*}\delta_{m,0}.$$

Similar expressions hold for the other odd and even metric elements, respectively.

APPENDIX B: COEFFICIENTS FOR GROWTH RATE SCALING

The coefficients for analytic growth rate scaling are given by

$$A_1(\theta)=\frac{\beta_0 p'}{(\psi')^2}\left(\frac{2\psi' q^2}{F}+\frac{1}{2}\rho(1+q^2)(1+E^2)\right)+(\gamma q/\psi')^2\tfrac{1}{2}(1+E^2)[1+s^2(\theta-\theta_k)^2],$$

$$A_2(\theta)=\beta_0 p' s(q/\psi')^2 X_M(\theta-\theta_k),$$

$$A_3(\theta)=\beta_0 p'(q/\psi')^2 X_M,$$

$$A_4(\theta)=[\beta_0 p'/2(\psi')^2]\rho(1+q^2)(1-E^2)s(\theta-\theta_k)+(\gamma q/\psi')^2 s(1-E^2)(\theta-\theta_k),$$

$$A_5(\theta)=[\beta_0 p'/2(\psi')^2]\rho(1+q^2)(1-E^2)+(\gamma q/\psi')^2\tfrac{1}{2}(1-E^2)[1-s^2(\theta-\theta_k)^2].$$

It is convenient to define

$$x=s(\theta-\theta_k),\quad u=\tfrac{1}{2}A_3,$$
$$a_1=\gamma a_r+A_1,\quad a_3=-A_4/(2x),$$
$$a_2=\tfrac{1}{2}A_5,\quad a_4=a_1+3\gamma a_r.$$

Then, the slowly varying amplitudes V_s, V_c, W_s, and W_c are given by

$$V_s=2uxV_0\phi_s/\Delta,\quad W_s=2V_0x\phi_{W_s}/\Delta,$$
$$V_c=2uV_0\phi_c/\Delta,\quad W_c=2V_0\phi_{W_c}/\Delta,$$

where

$$\Delta=a_4^2\{(a_1^2-a_2^2)-2(a_1/a_4)u^2(1+x^2)+[u(1+x^2)/a_4]^2-(a_3x)^2\},$$

$$\phi_s=a_4^2(a_2-a_1-a_3)+a_1a_4(a_2-a_3)-a_4a_2^2-a_3^2a_4x^2+u^2(1+x^2)(a_4+a_3-a_2),$$

$$\phi_c=-a_3a_4x^2(a_1+a_3+a_4)+u^2(1+x^2)\times(a_4+a_2+a_3x^2)-a_4(a_1+a_2)(a_4+a_2),$$

$$\phi_{W_s}=-2u^4(1+x^2)+u^2[2a_1a_4-a_1a_3+a_3a_4+2a_2^2+a_3x^2(2a_3+a_4-a_1)]+a_3a_4(a_1^2-a_2^2)-a_3^3a_4x^2,$$

$$\phi_{W_c}=u^4(x^4-1)+u^2(a_2^2+a_2a_4+a_4a_1-a_1a_2)-u^2x^4a_3^2+u^2x^2(a_3^2-a_2^2+a_2a_4-a_1a_2-a_1a_4)+a_2a_4(a_1^2-a_2^2)-a_4a_2a_3^2x^2.$$

With this notation, the equation for V_0 becomes

$$a_r\gamma V_0^{\parallel}=(1/\Delta)[(a_1-\gamma a_r)\Delta+2u^2x^2\phi_s+2u^2\phi_c-2x^2a_3\phi_{W_s}-2a_2\phi_{W_c}].$$

The large x behavior of this equation is given by Eq. (57), where

$$c_1=-\frac{\Sigma}{\gamma a_r}\left(\frac{\psi'}{\gamma q}\right)^2\left(\frac{1+E^2}{2}\right)^{-4}\times\{1-\tfrac{1}{4}[(1-E^2)/(1+E^2)]^2\}^{-1},$$

$$c_2=\frac{\gamma}{a_r}\left(\frac{qs}{\psi'}\right)^2\left[1-\frac{1}{2}\left(\frac{1-E^2}{1+E^2}\right)^2\right]\left(\frac{1+E^2}{2}\right).$$

Denoting by

$$g_1(E)=2\left(\frac{1+E^2}{2}\right)^3+\left(\frac{1+E^2}{2}\right)\left(\frac{1-E^2}{4}\right)^2-3\left(\frac{1-E^2}{4}\right)^2\left(\frac{1+E^2}{2}\right)^2-\left(\frac{1-E^2}{4}\right)^3,$$

$$g_2(E)=5\left(\frac{1+E^2}{2}\right)^4-10\left(\frac{1+E^2}{2}\right)^2\left(\frac{1-E^2}{4}\right)^2+4\left(\frac{1-E^2}{4}\right)^4,$$

$$g_3(E)=\left(\frac{1-E^2}{4}\right)^2\left(\frac{1+E^2}{2}\right)\times\left[3\left(\frac{1+E^2}{2}\right)^2-4\left(\frac{1-E^2}{4}\right)^2\right],$$

$$g_4(E)=\left(\frac{1+E^2}{2}\right)\left[5\left(\frac{1+E^2}{2}\right)^4+10\left(\frac{1-E^2}{4}\right)^4-15\left(\frac{1+E^2}{2}\right)^2\left(\frac{1-E^2}{4}\right)^2\right],$$

$$g_5(E)=5\left(\frac{1+E^2}{2}\right)^4+2\left(\frac{1-E^2}{4}\right)^4-9\left(\frac{1-E^2}{4}\right)^2\left(\frac{1+E^2}{2}\right)^2,$$

the expression for Σ is

$$\Sigma=-\frac{1}{2}\left[\beta_0 p' X_M\left(\frac{q}{\psi'}\right)^2\right]^2 g_1(E)+2\gamma a_r\left(\frac{\gamma q}{\psi'}\right)^2 g_2(E)-[\beta_0 p'\rho(1+q^2)/(\psi')^2]^2 g_3(E)+(\gamma q/\psi')^4 g_4(E)+(\gamma q/\psi')^2\times[\beta_0 p'/(\psi')^2][\rho(1+q^2)g_4(E)-2q^2(\psi'/F)g_5(E)].$$

Finally, the f_i's are given by

$$f_1(E)=\frac{g_1(E)}{g_2(E)},\quad f_2(E)=\frac{2g_3(E)}{g_2(E)}.$$

[1] J. L. Johnson, C. R. Oberman, R. M. Kulsrud, and E. A. Frieman, in *Proceedings of the Second International Conference on the Peaceful Uses of Atomic Energy* (United Nations, Geneva, 1958), Vol. 31, p. 198.
[2] R. Gruber, S. Semenzato, F. Troyon, T. Tsunematsu, W. Kerner, P. Merkel, and W. Schneider, Comput. Phys. Commun. **24**, 363 (1981).
[3] P. Merkel, J. Nührenberg, R. Gruber, and F. Troyon, Nucl. Fusion **23**, 1061 (1983).
[4] M. Mond, Phys. Fluids **26**, 3327 (1983).
[5] D. A. Monticello, R. L. Dewar, H. P. Furth, and A. Reiman, Phys. Fluids **27**, 1248 (1984).
[6] D. C. Barnes and J. R. Cary, Phys. Fluids **27**, 2522 (1984).
[7] J. W. Connor, R. J. Hastie, and J. B. Taylor, Proc. R. Soc. London A **365**, 1 (1979).

[8]H. L. Berk, M. N. Rosenbluth, and J. L. Shohet, Phys. Fluids **26**, 2616 (1983).
[9]B. B. Kadomtsev, Sov. Phys. JETP **10**, 962 (1960).
[10]F. A. Haas, Nucl. Fusion **15**, 407 (1975).
[11]D. Correa-Restrepo, Z. Naturforsch. **37a**, 848 (1982).
[12]K. Harafuji, N. Sasaki, H. Watanabe, and S. Nagao, J. Phys. Soc. Jpn. **48**, 1323 (1980).
[13]F. L. Ribe, G. C. Harper, M. Cekic, C. M. Greenfield, E. Hedin, and M. Koepke, Bull. Am. Phys. Soc. **29**, 1250 (1984).
[14]H. R. Strauss, Phys. Fluids **24**, 2004 (1981).
[15]W. A. Cooper and M. C. Depassier, Phys. Rev. A **32**, 3124 (1985).
[16]T. C. Hender, B. A. Carreras, W. A. Cooper, J. A. Holmes, P. H. Diamond, and P. L. Similon, Phys. Fluids **27**, 1439 (1984).
[17]B. A. Carreras, P. H. Diamond, M. Murakami, J. L. Dunlap, J. D. Bell, H. R. Hicks, J. A. Holmes, E. A. Lazarus, V. K. Paré, P. Similon, C. E. Thomas, and R. M. Wieland, Phys. Rev. Lett. **50**, 503 (1983).
[18]B. Coppi, J. M. Greene, and J. L. Johnson, Nucl. Fusion **6**, 101 (1966).
[19]J. L. Johnson and J. M. Greene, Plasma Phys. **9**, 611 (1967).